

Zeitschrift: IABSE reports of the working commissions = Rapports des commissions de travail AIPC = IVBH Berichte der Arbeitskommissionen
Band: 13 (1973)
Artikel: Plastic H-columns under repeated biaxial loading
Autor: Chen, W.F.
DOI: <https://doi.org/10.5169/seals-13739>

Nutzungsbedingungen

Die ETH-Bibliothek ist die Anbieterin der digitalisierten Zeitschriften. Sie besitzt keine Urheberrechte an den Zeitschriften und ist nicht verantwortlich für deren Inhalte. Die Rechte liegen in der Regel bei den Herausgebern beziehungsweise den externen Rechteinhabern. [Siehe Rechtliche Hinweise.](#)

Conditions d'utilisation

L'ETH Library est le fournisseur des revues numérisées. Elle ne détient aucun droit d'auteur sur les revues et n'est pas responsable de leur contenu. En règle générale, les droits sont détenus par les éditeurs ou les détenteurs de droits externes. [Voir Informations légales.](#)

Terms of use

The ETH Library is the provider of the digitised journals. It does not own any copyrights to the journals and is not responsible for their content. The rights usually lie with the publishers or the external rights holders. [See Legal notice.](#)

Download PDF: 15.05.2025

ETH-Bibliothek Zürich, E-Periodica, <https://www.e-periodica.ch>

Plastic H-Columns Under Repeated Biaxial Loading

Colonnes plastiques à profils H soumises à des charges répétées biaxiales

Plastische Stützen mit H-Querschnitt unter wiederholter zweiachsigter Belastung

W.F. CHEN

Associate Professor
Department of Civil Engineering
Fritz Engineering Laboratory
Lehigh University
Bethlehem, Pennsylvania
USA

INTRODUCTION: Moment-curvature-thrust relationships are of prime importance in any analysis of structural behavior. For a biaxially loaded steel H-column, the appropriate set of loadings are bending moments M_x and M_y , axial force P and warping moment M_{xy} . The corresponding set of deformations are bending curvatures, ϕ_x and ϕ_y , axial strain ϵ and warping curvature ϕ_{xy} . This may be demonstrated clearly by considering a simple physical model as shown in Fig. 1. The biaxial load is seen to be decomposed into four components. The first three are statically equivalent to an axial force $4P$ and two bending moments M_x and M_y about two principal axis of the H-section. However, these three equivalent systems do not produce the biaxial load $4P$. It is necessary to consider a fourth system which produces zero axial force and zero bending moment resultants on the section. This fourth system termed warping moment, M_{xy} , causes the column to warp or twist.

For the most part, plastic analysis and design of biaxially loaded columns have in the past been directed toward the study of proportional, monotonically increasing loading to failure [1]. This type of loading is not entirely realistic for many applications, however. Herein a study is made of the relationships between moments and curvatures for a relatively short steel column subject to repeated and reversed compression combined with biaxial bending moments.

The term relatively "short" steel columns referred to here means that the effect of lateral deflections on the magnitudes of bending moment is negligible. Furthermore, effects of local buckling are not included in the analysis.

STRESS-STRAIN RELATIONSHIPS INCLUDING HYSTERESIS: The stress-strain relationship is assumed to be tri-linear as shown in Fig. 2. The curve is composed of three regimes: elastic; plastic; and strain hardening. The plastic unloading behavior is idealized as shown in the figure. If the material is unloaded from the plastic regime, the material exhibits no Bauschinger effect. However, if the material is unloaded from the strain hardening regime, some Bauschinger effects are exhibited. This strain hardening, plastic unloading rule and Bauschinger effect are interpreted clearly by the kinematic model of the parallelogram $BD'B'D$ and the straight line AA' (Fig. 2). Elastic loading or plastic unloading within the line AA' does not change the condition at all (Fig. 2a). Plastic loading along lines DB or $D'B'$ changes the position of line AA' only (Fig. 2b). Strain hardening along lines BC or $B'C'$ translates the position of the parallelogram $BD'B'D$ in parallel to the lines BC and $B'C'$ (Fig. 2c). In this case, the elastic line AA' coincides with the line BD' . Positions of the lines BC and $B'C'$ do not change for any loading history.

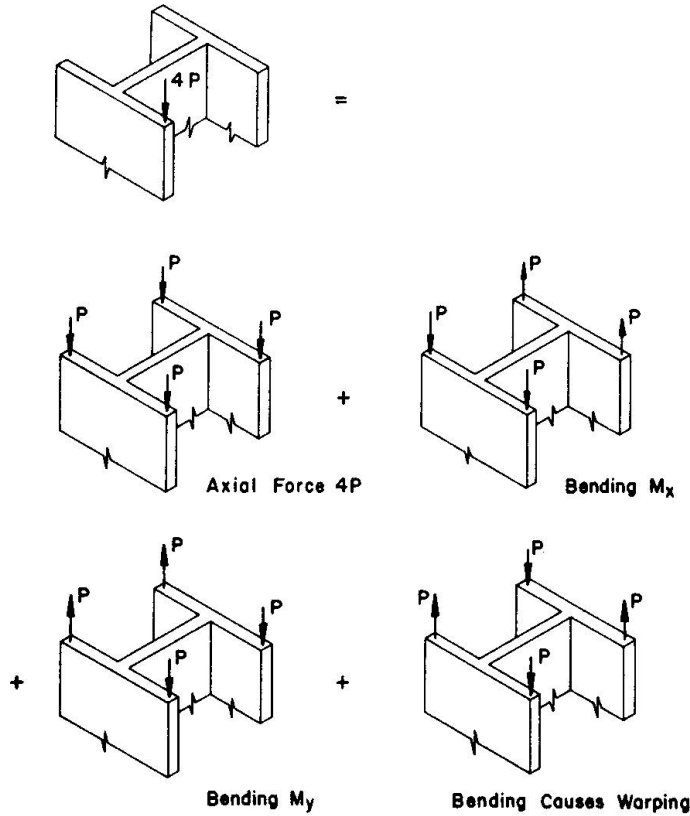


Fig. 1 Decomposition of a Biaxial Loading

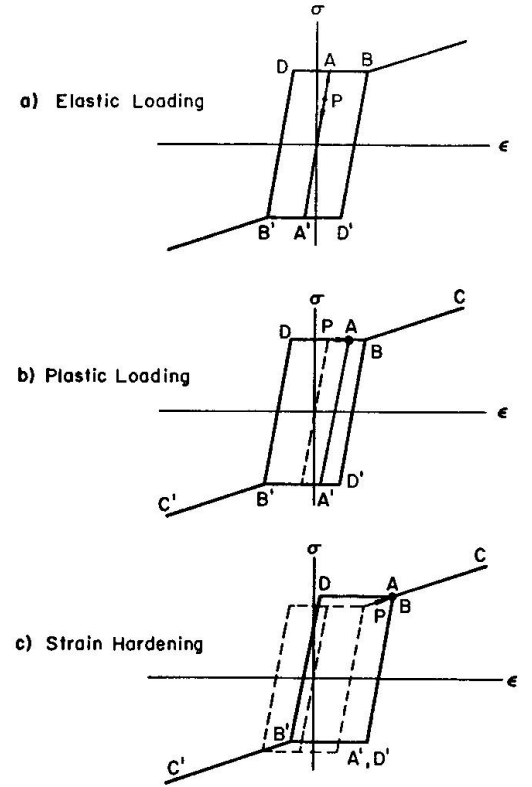


Fig. 2 Stress-Strain Model

MATHEMATICAL FORMULATION: Since only normal stress and normal strain are considered, deformation quantities related to normal strain are taken as generalized strains of the H-section. This results in the following relationship between the generalized strain $\{\delta\}$ and the strain, ϵ :

$$\{\delta\} = \begin{Bmatrix} \epsilon_o \\ \varphi_x \\ \varphi_y \\ \varphi_{xy} \end{Bmatrix} = \begin{Bmatrix} \frac{1}{A} \int dA \\ \frac{1}{A} \int \frac{\partial \epsilon}{\partial y} dA \\ \frac{1}{A} \int \frac{\partial \epsilon}{\partial x} dA \\ \frac{1}{A} \int \frac{\partial^2 \epsilon}{\partial x \partial y} dA \end{Bmatrix} \quad \begin{array}{l} \text{strain at centroid} \\ \text{curvature about x-axis} \\ \text{curvature about y-axis} \\ \text{warping curvature about the centroid} \end{array} \quad (1)$$

Strain distribution is assumed to be linear in x and y coordinate.

$$\epsilon = \epsilon_o + x \varphi_y + y \varphi_x + xy \varphi_{xy} \quad (2)$$

The corresponding resultant forces or generalized stresses are determined from the rate of internal energy dissipation

$$\dot{D}_I = \int \sigma \dot{\epsilon} dA = \dot{\epsilon}_o \int \sigma dA + \dot{\varphi}_x \int \sigma y dA + \dot{\varphi}_y \int \sigma x dA + \dot{\varphi}_{xy} \int \sigma xy dA \quad (3)$$

This results in the following relationship between the generalized stress $\{f\}$ and the stress, σ :

$$\{f\} = \begin{Bmatrix} P \\ M_x \\ M_y \\ M_{xy} \end{Bmatrix} = \begin{Bmatrix} \int \sigma dA \\ \int \sigma y dA \\ \int \sigma x dA \\ \int \sigma xy dA \end{Bmatrix} \quad \begin{array}{l} \text{axial thrust} \\ \text{bending moment about x-axis} \\ \text{bending moment about y-axis} \\ \text{warping moment about the centroid} \end{array} \quad (4)$$

Because plastic behavior is load path dependent and usually requires step-by-step calculations that follows the history of loading. For this reason, it has proven useful to establish an analytical relationship of the generalized stress-strain or moment-curvature relation in terms of the incremental changes of $\{df\}$ and $\{d\delta\}$. This leads to the linear relationship between these quantities

$$\{df\} = [K] \{d\delta\} \quad (5)$$

The matrix $[K]$ is defined as the tangent stiffness matrix as it represents the tangent of the generalized stress-strain curve as well as the stiffness of the cross section. A detailed description on the analytical derivation of this equation is given in Ref. 2.

METHOD OF SOLUTION: The numerical solution of Eq. 5 can be obtained by the tangent stiffness method. Details of the method have been given in Ref. 3 for a relatively short column and in Ref. 4 for the case of a long column: A brief description of the tangent stiffness method will be given herein.

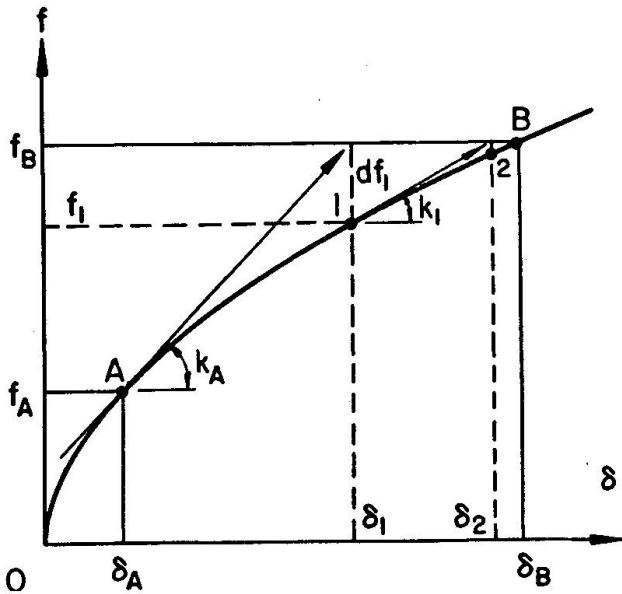


Fig. 3 Tangent Stiffness Method

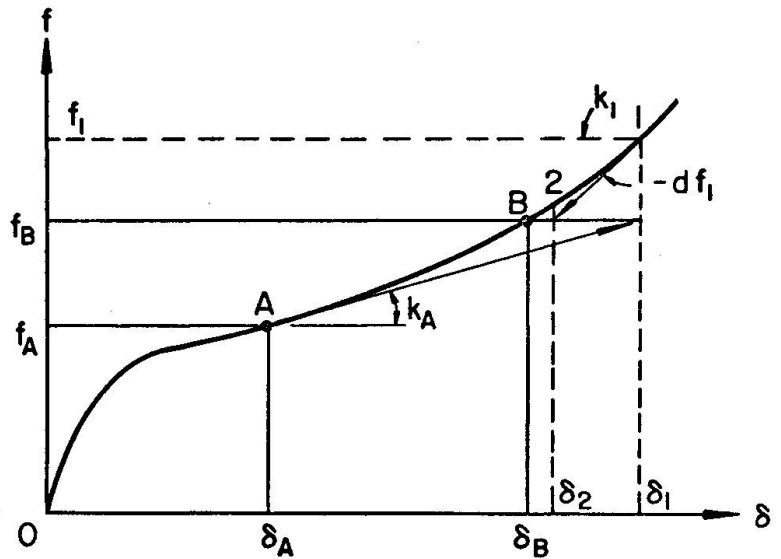


Fig. 4 Tangent Stiffness Method with Strain Hardening

Consider a generalized stress or a force vector f , a generalized strain or a deformation vector δ and their relationship is shown in Fig. 3. The column segment has experienced loadings along the path OA. At point A, the current force vector f_A , deformation vector δ_A and the stiffness matrix K_A are assumed to be known, the problem is to find the corresponding deformation vector δ_B when the force vector is increased from f_A to f_B .

Since the deformation increment $d\delta$ can be calculated from the force increment df or $df = f_B - f_A$ using the tangent stiffness K_A at the current state A, or $d\delta_1 = K_A^{-1} df$. The first approximate value of total deformation is obtained by $\delta_1 = \delta_A + d\delta_1$. From this approximate deformation δ_1 , the total strain distribution ϵ can be determined from Eq. 2 and hence the corresponding state of stress can be determined. Integration of the stress over the entire cross section gives the new internal force vector f_1 using Eq. 4. This new state is expressed by the point 1 in Fig. 3. The new tangent stiffness K_1 at point 1 corresponding to the state f_1 and δ_1 can now be computed. The new internal force vector f_1 is now not in equilibrium with the externally applied force vector f_B . The first unbalanced force vector df_1 is computed from $df_1 = f_B - f_1$.

The next step is to find a correction deformation vector $d\delta_2$ which will be added to δ_1 in order to eliminate the unbalance force f_1 . Vector $d\delta_2 = K_1^{-1} df_1$. Repeating the same procedure for point 2 again, the second internal force vector f_2 and the unbalanced force vector $df_2 = f_B - f_2$ are obtained. Repeating the

same procedure as at point 2 until the unbalanced force df at point n becomes zero or is within a prescribed tolerance limit, the final deformation vector is then obtained by $\delta_B \approx \delta_n$.

During the procedure, the unbalance force vector df may be negative as shown in Fig. 4. This happens when there is some strain hardening in the material. In such a case, tangent stiffness rather than elastic unloading stiffness should be used in the computations because this negative force vector is an imaginary unloading.

In most cases, a few cycles of iteration are found to be sufficient to obtain an accurate solution. Even with a large incremental force or a rather accurate calculation of large deformation on a plastic plateau the solution will generally converge within just a few more cycles of iteration.

HYSTERESIS DIAGRAMS: The moment-curvature diagrams for a column segment contain considerable information about the behavior of a biaxially loaded long column. In addition to providing the essential relationship between forces and deformations for a long column solution, the diagrams make it possible to determine the energy input to the segment through integration of the work done by the external forces.

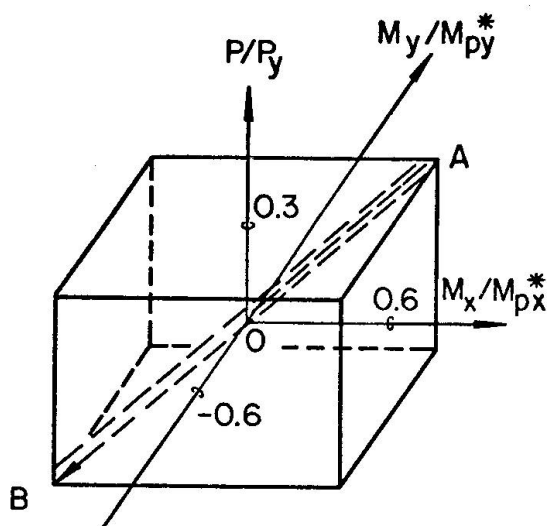


Fig. 5 Repeated and Reversed Proportional Loading

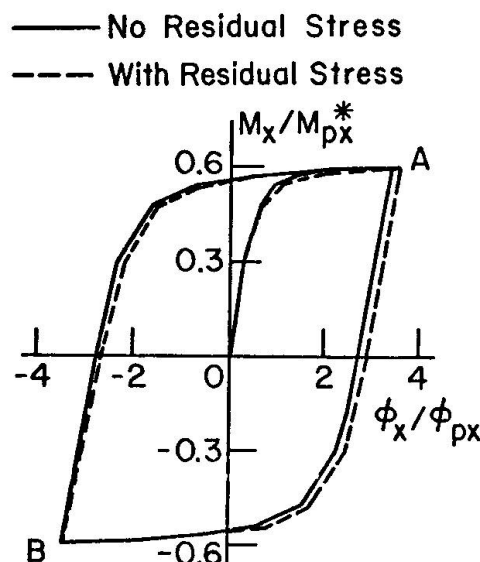


Fig. 6 Moment-Curvature Hysteresis Diagram

Figure 5 shows a proportional loading case with the loads (P, M_x, M_y) being repeated and reversed proportionally between 99% (point A) and -99% (point B) of the values $(0.3, 0.6, 0.6)$ of the full plastic limit state $(P_y, M_{px}^*, M_{py}^*)$. Linear strain hardening and linear residual stress distributions are considered but the warping deformation ϕ_{xy} is assumed to be completely restrained, the corresponding warping moment M_{xy} required for such a restraint is therefore considered as a reaction. Its magnitude is found to be the same at points A and B. The presence of residual stress is seen to have some effects on the moment-curvature curves as shown by the typical example of M_x vs. ϕ_x curve in Fig. 6, but the effect of material strain hardening on the curves is found to be not significant.

The typical moment-curvature hysteresis loop shown in Fig. 6 is composed of three portions: initial loading portion ($0 \rightarrow A$), unloading ($A \rightarrow B$), and reloading portion ($B \rightarrow A$). For each portion, a function similar to a Ramberg-Osgood type of function may be used for curve-fitting. As an example, Fig. 7 shows a typical example of the close curve-fitting for the M_x vs. ϕ_x curve discussed in Fig. 6. The Ramberg-Osgood function for the initial loading portion is shown on the top of the figure. The functions for the unloading portion and reloading portion are identical in shape to the function shown, but enlarged by a factor of two and shifting the origin.

RESPONSE TO REPEATED AND REVERSED LOADING: Response of section under repeated and reversed loadings is of major importance in the low-cycle fatigue and shake-down analysis. In these analyses, estimation of energy dissipation during the loading cycle plays an important role.

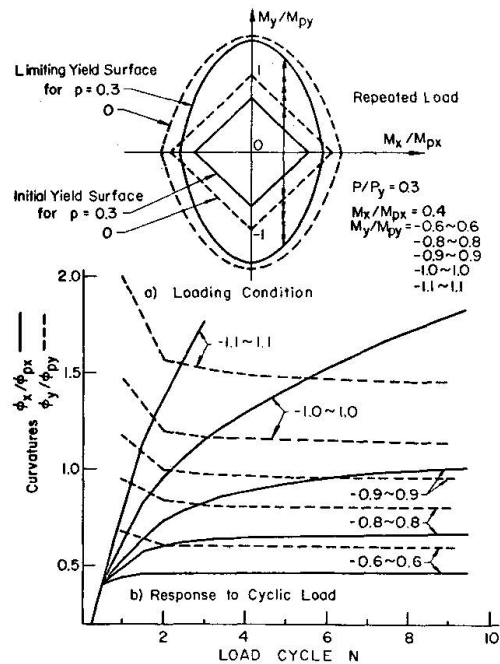
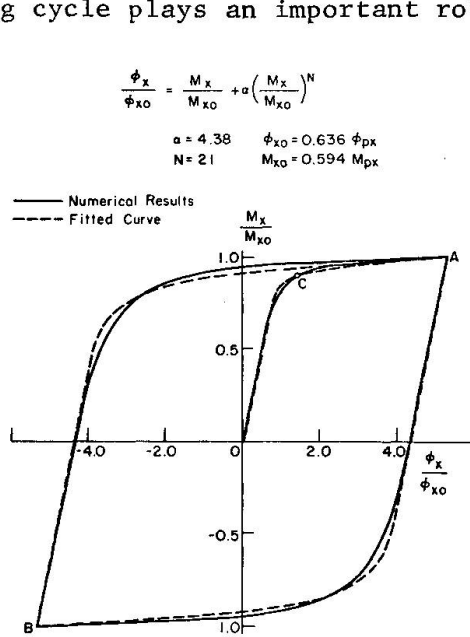


Fig. 7 Curve-Fitting by Ramberg-Osgood Type of Function Fig. 8 Repeated and Reversed Non-Proportional Loading

Figure 8 shows the load M fluctuating between some limits while the other two loads are kept constant ($P/P_y = 0.3$, $M_x/M_{px} = 0.4$). The half amplitude of the limits for the moment M_y/M_{py} is 0.6, 0.8, 0.9, 1.0 and 1.1 (M_{px} and M_{py} denote initial yield values). Since the elastic region is bounded by $-0.3 \leq M_y/M_{py} \leq 0.3$, plastic deformations are produced in all cases. Numerical results are illustrated in Fig. 8. In all cases, curvature ϕ decreases with loading cycles and tends to converge to a certain limit value. The deformations ϵ and ϕ and the energy dissipation are found to increase monotonically with the loading cycles for large amplitudes but tend to converge for small amplitudes ($M_y/M_{py} < 1.0$).

SUBSEQUENT YIELD SURFACES: Since the loading condition is kept constant during the repetition of loadings, shakedown is possible only when the subsequent yield surface is transformed so that the loading points will eventually move within the yield surface.

Figure 9 shows subsequent yield surfaces due to loadings $P/P_y = 0$, $M_x/M_{px} = 0.4$ and M_y/M_{py} between 0.8 and -0.8. The dotted lines are the initial yield surface and the limiting yield surface. A load point inside and outside of the yield surface represent elastic and elastic-plastic states of stress, respectively. No load point can move outside the limiting surface.

After the first loading (point A), the yield surface translates so that the load point A is now on the subsequent yield surface. There are two interesting points: (1) The opposite side of point A moves towards the origin (Bauschinger Effect); (2) The subsequent yield surface has a corner at the loading point. After the second loading (point B), the subsequent yield surface changes again and both points A and B are now inside the surface. Thus the repetition of loading between A and B proceeds all in elastic regime and further plastic deformation has ceased, or the section has shaken down.

Figure 10 shows changes of the subsequent yield surface due to repeated and reversed loading $P/P_y = 0.3$, $M_x/M_{px} = 0.4$ and M_y/M_{py} between 1.1 and -1.1. The repeated loading M_y is applied between the points A and B. When the amplitude

of M_y is small ($M_y/M_{py} = 0.8$, Fig. 9) the subsequent yield surface tends to change so that the column segment shakes down. When the amplitude is large ($M_y/M_{py} = 1.1$, Fig. 10), the tendency of shakedown is not observed.

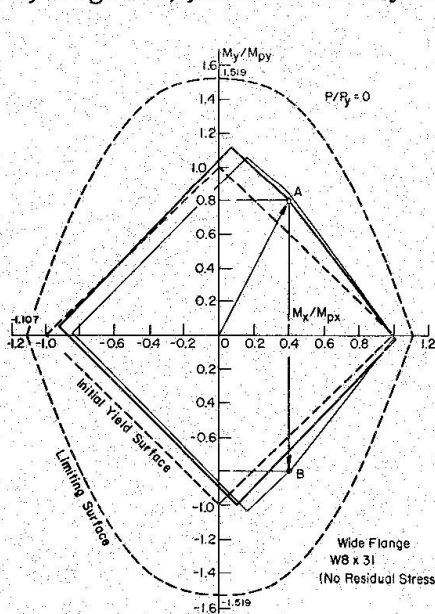


Fig. 9 Subsequent Yield Surface

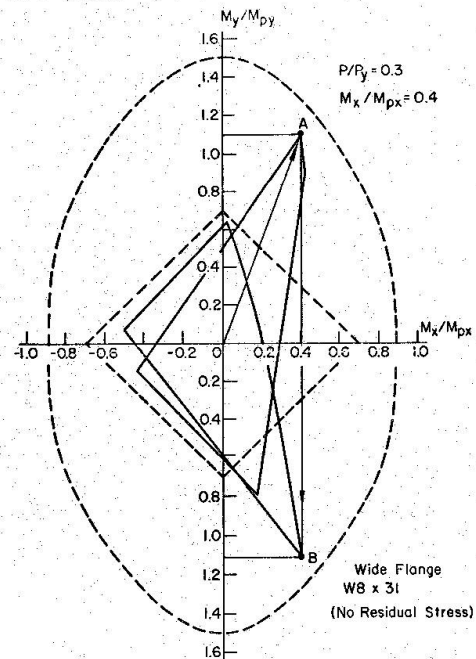


Fig. 10 Transformation of Subsequent Yield Surface

CONCLUSIONS: Based upon the formulation (Eq. 5), a computer program was developed to provide numerical results. It is found that (1) The method is extremely powerful and efficient for computer solutions of moment-curvature hysteresis loops; (2) The mathematical representation of a hysteresis moment-curvature curve using the Ramberg-Osgood relationship is highly satisfactory; and (3) The response of a column segment subjected to repeated and reversed biaxial loading and the concepts of a shakedown analysis can be interpreted from the viewpoint of transformation of the subsequent yield surfaces in the generalized stress space.

ACKNOWLEDGMENTS: The research reported here was supported by the National Science Foundation under Grant GK-35886 to Lehigh University.

REFERENCES:

1. Chen, W. F. and Santathadaporn, S., "Review of Column Behavior under Biaxial Loading", Journal of the Structural Division, ASCE, Vol. 94, No. ST12, Proc. paper 6316, December 1968, pp. 2999-3021.
2. Chen, W. F. and Atsuta, T., "Inelastic Response of Column Segments under Biaxial Loads", Journal of the Structural Division, ASCE, Vol. 99, 1973, (in press).
3. Santathadaporn, S. and Chen, W. F., "Tangent Stiffness Method for Biaxial Bending", Journal of the Structural Division, ASCE, Vol. 98, No. ST1, Proc. paper 8637, January 1972, pp. 153-163.
4. Santathadaporn, S. and Chen, W. F., "Analysis of Biaxially Loaded H-Columns", Journal of the Structural Division, ASCE, Vol. 99, ST3, March 1973, pp. 491-509.

SUMMARY

A study is made of the relationships between moments and curvatures for a relatively short steel H-column subject to repeated and reversed compression combined with biaxial bending moments. Plastic unloading, residual stresses, strain hardening and Bauschinger effect of the material are considered in the analysis. Moment-curvature curves corresponding to several repeated and reversed loading paths are presented.

RESUME

Dans ce rapport on étudie les relations moment-courbure pour une colonne à larges ailes en acier relativement courte, soumise à des efforts de compression répétés et alternés, combinés avec des moments de flexion biaxiaux. Le déchargement plastique, les tensions résiduelles, l'écrouissage et l'effet Bauschinger du matériau sont considérés dans l'analyse. On présente aussi certains diagrammes moment-courbure correspondant à plusieurs types de charges répétées et alternées.

ZUSAMMENFASSUNG

Es wird eine Untersuchung der Beziehung zwischen Moment und Krümmung einer relativ gedrunenen Stahlstütze mit H-Querschnitt unter wiederholter und wechselnder Last, kombiniert mit Biegemomenten in beiden Richtungen vorgelegt. Plastische Entlastung, bleibende Spannungen und der Bauschinger-Effekt werden in der Berechnung berücksichtigt, und Momenten-Krümmungs-Kurven entsprechend wiederholter und wechselnder Belastungen gezeigt.

Leere Seite
Blank page
Page vide